16th World Conference on Earthquake, 16WCEE 2017
Santiago Chile, January 9th to 13th 2017
Paper N° 503 (Abstract ID)
Registration Code: S-O1461068398

ASSESSING TSUNAMI RISK TO KARACHI PORT THROUGH SIMULATION OF CURRENTS THAT WERE REPORTEDLY PRODUCED THERE BY THE 1945 MAKRAN TSUNAMI

H. Hasan[(1)], H. A. Lodhi[(2)], R. J. LeVeque[(3)], S. H. Lodi[(4)], S. Ahmed[(5)]

[(1)] *Associate Professor, Department of Civil Engineering, NED University of Engineering and Technology, hhasan@neduet.edu.pk*
[(2)] *Lecturer, Department of Physics, NED University of Engineering and Technology, hiralodi@neduet.edu.pk*
[(3)] *Professor, Department of Applied Mathematics, University of Washington, rjl@uw.edu*
[(4)] *Professor, Department of Civil Engineering, NED University of Engineering and Technology, sarosh.lodi@neduet.edu.pk*
[(5)] *Lecturer, Department of Civil Engineering, NED University of Engineering and Technology, shoaibahmed@neduet.edu.pk*

Abstract

A train of tsunami waves, by resembling a swift series of tides, can produce damaging currents even where wave heights are modest. At Karachi Port, the 1945 Makran tsunami moved boats and damaged a rock groyne without exceeding 3 m in height above ambient tide. A newspaper account mentions an ebb current of 4 to 5 knots. We obtained ebb currents in this range by means of computer simulations with GeoClaw, an open-source code. The simulations, which use bathymetry and shorelines mapped before 1945, presuppose for simplicity a purely tectonic source for the 1945 tsunami. The simulations were tested mainly against an incomplete marigram from the Karachi tide gauge. Runs with modern bathymetry and shorelines show weaker currents, probably because of a post-1945 extension of a breakwater. Using a damage index previously developed from tsunami-current measurements in other harbours, we asked whether the currents simulated for 1945 were fast enough to cause the reported damage to the groyne. Those currents were found fast enough to have caused damage termed “Minor/Moderate” in seaward parts of Karachi Harbour.

Keywords: tsunami; current speeds; Makran; Karachi Port

1. Introduction

Tsunami currents can cause damage in ports and harbours even without flooding the adjacent land. The currents may turn vessels and dockside cargo into battering rams, which may in turn damage docks and quay walls. Measurements of current velocities have been obtained for both near-field and far-field tsunami effects on maritime facilities worldwide, for use in modelling tsunami-induced currents, including eddies, in harbour basins [1]. Television footage showed large turbulent eddies during the 2011 Tohoku tsunami in northeast Japan. Ships in port were moved by far-field waves of the 2004 Indian Ocean tsunami in Salalah, Oman [2], and by near-field waves of a slide-induced tsunami in 1964 at Valdez, Alaska [3].

The main tsunami threat in Pakistan, as in Japan, is posed by waves generated nearby. The largest nearby source of tsunamis in Pakistan is an active fault at the boundary between two tectonic plates. This plate boundary fault is a gently inclined thrust, dipping northward, that extends 800 km east-west along the Makran Subduction Zone. The western part of the subduction thrust slants beneath southeast Iran and may present a tsunami hazard in nearby parts of Oman (see Fig. 1).

The largest earthquake unquestionably produced on the Makran subduction thrust took place just over 70 years ago. The earthquake source area was a few hundred kilometres west of Karachi. The fault rupture began offshore Pasni early on November 28, 1945, Indian Standard Time (at 2156:55.2 UTC [4]). From that starting point (hypocenter) the fault rupture is believed to have spread 100-150 km eastward to the vicinity of Ormara. Byrne et al. [4] using Rayleigh waves, obtained moment magnitudes in the range 8.0–8.2, and reported 8.1 as the best estimate.

The earthquake was followed by a tsunami of ambiguous origin that caused hundreds of confirmed fatalities and entered the Port of Karachi. The tsunami has been ascribed to vertical tectonic deformation of the ocean floor during the earthquake [5], but submarine slides may have also contributed to the waves [4,6,7]. Nearly all the confirmed tsunami deaths were in what is now Pakistan, and about half were east of Karachi in the Indus River delta [8–11]. Flooding and damage in Karachi Harbour are known from contemporary newspaper reports and from recent interviews with eyewitnesses. Front-page articles in two of Karachi's dailies of the time, *The Sind Observer* and *The Daily Gazette*, described flooding of compounds of the port's oil installations at Keamari; damage to 400 feet of a groyne that was then under repair; and loss of a beacon light. The groyne damaged was a stone structure constructed in 1861-1863 [12]. Eyewitness interviewed in the past few years have told of flooding on low-lying Baba Island and Bhit Islands, and also the grounding of a Gujarati ship [11].

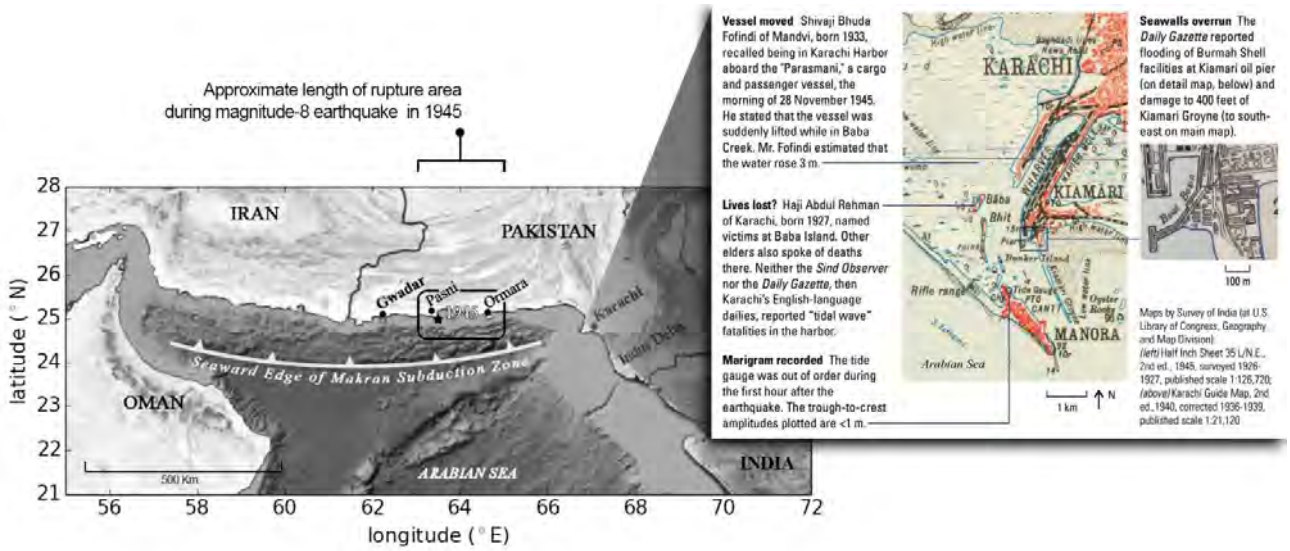

Fig. 1 – Approximate source of the 1945 Makran earthquake [4] and tsunami effects in Karachi [10]

We posit in this paper that these tsunami effects in the Karachi Harbour resulted from the tsunami currents rather than high water levels. Strong currents were reported in *The Times of India*, which on November 30 told of "a strong ebbing current of 4 to 5 knots" in Karachi Harbour. The *Times* account, citing a news service (A.P.I.) as its source, mentions four waves in the harbour: the first at 5:30 am, the bigger second one at 7 am followed by the third at 7:50 am, and the fourth and highest at 8:15 am. This same sequence was

reiterated in official reports by Pendse [13,14]. Multiple waves are further evidenced by an incomplete marigram from a float-type tide gauge that had been installed before 2nd January 1924 at a pier along the shore of Manora Island. The marigram lacks data from the first 75 minutes after the earthquake [7], and the amplitudes of the waves recorded are smaller than those evidenced by accounts of flooding and damage.

It is important to understand the currents of 1945 as guides to tsunami hazards in today's Port of Karachi. This paper accordingly examines the 1945 tsunami at Karachi by simulating it with an open-source code, GeoClaw, and by comparing the simulated wave train and currents with the observations summarized above. The simulations incorporate debatable assumptions about sources for the 1945 tsunami. We compute current speeds for two terrain models—one using bathymetry and shorelines surveyed before 1945, the other using recent surveys. With the earlier terrain we ask whether the simulated current speeds could account for the damage reported in 1945. With the newer terrain we apply a damage index previously developed from tsunami-current measurements in harbours and ports worldwide [15], as a preliminary guide to tsunami risk to modern maritime facilities at Karachi Port.

2. Numerical Model Setup

We simulated current speeds with an open-source code, GeoClaw [16], that was developed as part of Clawpack [17]. The program uses a high-resolution shock capturing finite-volume method to solve the depth-averaged two-dimensional nonlinear shallow water equations that are standard in modelling tsunami propagation and inundation. Geoclaw improves on some other tsunami-modelling codes by allowing for efficient solution of modelling problems through adaptive mesh refinement. In adaptive mesh refinement, fine computational grids are used only where needed, such as when handling the inundation on land through wetting and drying algorithms. Additional levels of refinement can be introduced in specific coastal regions as the wave arrives. The code allows parallel processing to attain additional speed on multi-core computers and has the advantage that the digital elevation models (DEMs) for bathymetry and topography can be provided arbitrarily at different resolutions. Arbitrarily complex topography and shorelines can be incorporated without the need for mesh generation since the computations are done on rectangular grid cells in longitude-latitude.

2.1 Digital Elevation Models (DEMs) for Karachi Port

We made two DEMs for Karachi Port: one to approximate conditions in 1945, the other to represent the present-day situation. For both we drew on nautical charts for Karachi Port. Bathymetry surveyed before 1945 is available in a British Admiralty Chart published in 1935 with small corrections in 1939 [18] (see Fig. 2). Notes on the chart state that it is based on surveys of the outer soundings and the parts in hairline conducted by Navigating Lieutenant T.C. Pascoe under supervision of Commander L.S. Dawson from Royal Navy in 1883, and on further surveys by the Karachi Port Engineers to 1933, with small corrections in the years 1935, 1936, 1937 and 1939. For present-day conditions we used the 2012 edition [19] of a nautical chart that was first published in 1997. We are uncertain when the soundings used in this map were obtained. The chart mentions Notices to Mariners for years 2013 and 2014 but is not clear whether those notices refer to corrections.

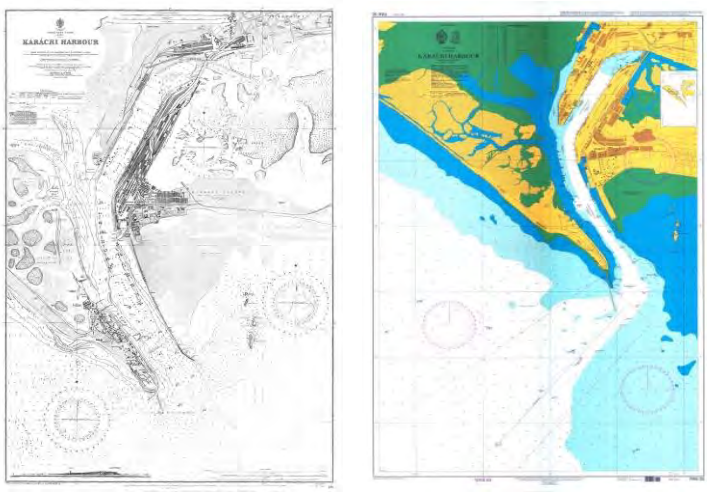

Fig. 2 - Nautical charts from 1939 [18] (left panel) and 2012 [19] (right panel)

Comparison between the two charts reflects expansion of Karachi Port since 1945. The changes include port protection structures and bathymetry in seaward parts of the harbour. The channel has been dredged deeper and the island just inside the channel has most likely been removed to make way for larger ships. These changes with time would have surely affected the alignment of the shoreline and wave dynamics inside the port including wave-generated currents. To capture these effects, two separate digital elevation models (DEMs) were developed—one with the bathymetric data compiled in 1939, the other with the 2012 chart. The earlier DEM also incorporates shoreline and topographic data from the 1944 edition on the Karachi Guide Map, by the Survey of India. The 1939 nautical chart shows a training groyne that we neglected because it is not seen in the guide map (see zoomed image of Karachi Port in Fig. 1). The nautical charts of 1939 and 2012 were digitised separately and mosaicked with the SRTM 30m topographic data (see Fig. 3). For offshore data other than Karachi Port, GEBCO bathymetric data was used together with nearshore bathymetric charts by US Defense Mapping Agency from the period 1994 to 2001.

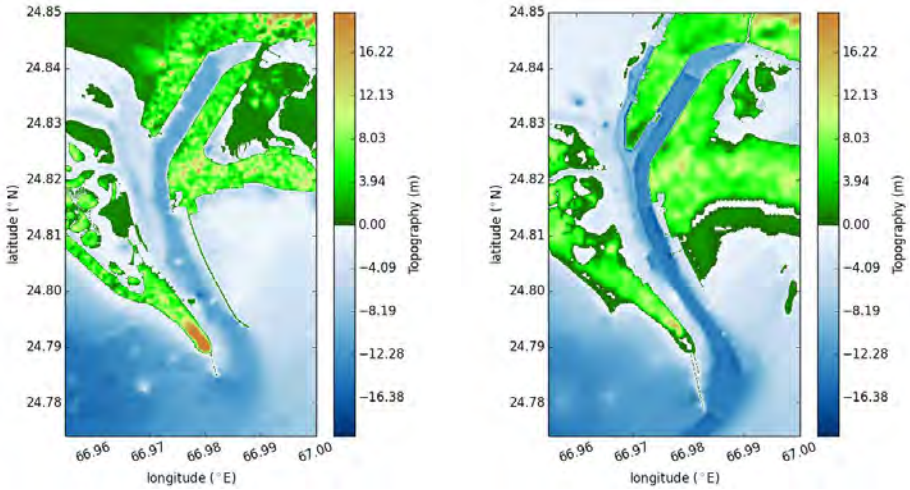

Fig. 3 – Digital Elevation Model for Karachi port using Nautical Charts for the years 1939 (left panel) and 2012 (right panel)

2.2 Previously Inferred Sources of the Great Makran Earthquake of 1945

The source of the great 1945 earthquake has been reported as a hypocenter and as a fault-rupture area. The fault rupture began at the hypocenter. The distinction is important in modelling of the 1945 tsunami, because the tsunami source, if purely from tectonic deformation, would be the warping of the ocean floor by tectonic deformation from coseismic slip wherever the fault broke.

Both the hypocenter and the fault-rupture area were evaluated by Byrne et al. [4]. Their Table 1, citing previous work, located the hypocenter offshore Pasni (lat. 24.15 N, long. 63.48 W) and gave its depth as 27 km. They reported a hypocenter and a nodal plane striking northeast-southwest (246°) and a slip direction nearly perpendicular to this strike (rake 89°). In their text, Byrne et al. [4] proceeded to derive estimates of the fault-rupture area and of the coseismic slip that occurred on it. Their Figure 6 sketches the long dimension of the rupture area (see Fig. 1) as parallel to the roughly east-west strike of the subduction thrust [4]. They inferred that the fault rupture area extended beneath Ormara, to account for reports that a shoreline there was raised about 2 m during the earthquake [20]. They recognized that subsidence reported from Pasni was probably induced by a landslide, but they extended the inferred fault-rupture area beneath Pasni as well. They concluded (p. 466–468) that the fault rupture extended 100-150 km along a plane dipping 5° north, that most of this area was east of Pasni, and that the rupture extended as much as 100 km down the gentle northward dip of the fault plane.

These estimates of hypocenter and fault-rupture area are conflated in some of the subsequent attempts to simulate the 1945 tsunami, ours included. The most recent of the simulations have been calibrated to tide-gauge data from marigrams in Karachi and Bombay [5,7]. In the most comprehensive modelling, by Heidarzadeh and Satake [5], the tide-gauge data were found to be consistent with an earthquake source represented by four rectangular segments, each with its own average slip (see Table 1). Each segment was

assumed to strike 246°, in agreement with the hypocentral solution in [4], but not with the more nearly east-west fault-rupture area inferred in [4]. Reference [9] describes each segment as having the same depth to its up-dip edge. It is not clear to us how to project these segments onto a subduction thrust that strikes close to 270°.

Table 1 – Source parameters for the Great Makran Earthquake of 1945 inferred from recent tsunami modelling [5]

Scenario		*South-east corner*									
		Long. (° E)	*Lat. (° N)*	*Fault Length (km)*	*Fault Width (km)*	*Upper Depth (km)*	*Slip (m)*	*Strike (°)*	*Rake (°)*	*Dip (°)*	*Mw*
Four segment fault	A	63.22	24.17	55	70	27	10.0	246	89	7	
	B	63.72	24.38	55	70	27	10.0	246	89	7	
	C	64.22	24.59	55	70	27	0.0	246	89	7	
	D	64.72	24.80	55	70	27	4.3	246	89	7	
Total/Average				220	70	27	6.1	246	89	7	8.28

2.3 Scenarios used in this report

Our preliminary simulations use two hypothetical sources. In both of these scenarios the fault rupture strikes 246°, oblique to the subduction thrust. Scenario 1 adapts the fault-rupture area of Byrne et al. [4] to this strike by rotating the strike about 25° counterclockwise. Scenario 2 follows the preferred fault rupture of Heidarzadeh and Satake [5], the four-segment hypothesis summarized above in Table 1. Both scenarios appear to require about twice as much seismic moment as was estimated by Byrne et al. [4]. The 246° strike yields vertical tectonic deformation consistent with the reports that uplift occurred at Ormara and not at Pasni (Fig. 4). Neither scenario allows for the deformation pattern to be modified by splay faulting or by submarine slope failures.

Table 2 – Scenarios used in this report to simulate the 1945 Makran tsunami

Scenario		*Top center Coordinates*									
		Long. (° E)	*Lat. (° N)*	*Fault Length (km)*	*Fault Width (km)*	*Depth (km)*	*Slip (m)*	*Strike (°)*	*Rake (°)*	*Dip (°)*	*Mw*
1		64.25	24.75	150	100	27	7	246	89	7	8.38
2	Fault Segment										
	A	63.22	24.17	55	70	27	10.0	246	89	7	
	B	63.72	24.38	55	70	27	10.0	246	89	7	
	C	64.22	24.59	55	70	27	0.0	246	89	7	
	D	64.72	24.80	55	70	27	4.3	246	89	7	
	Total/Average			220	70	27	6.1	246	89	7	8.38

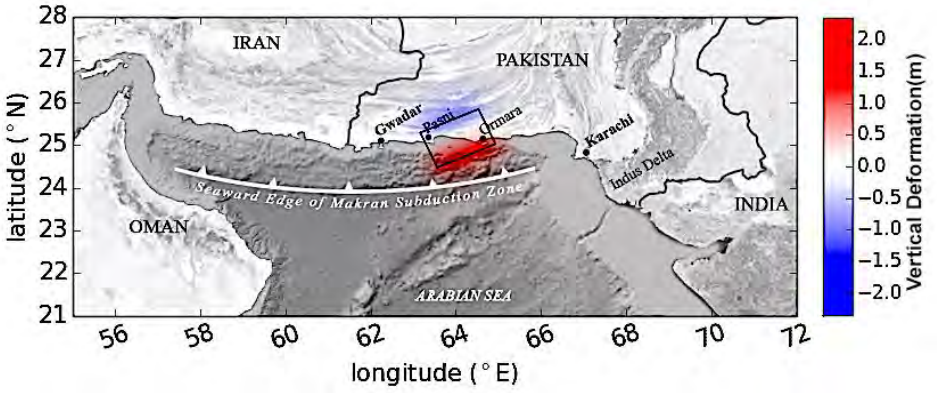

(a) Scenario 1 based on Byrne et al. (1992) [4] but with oblique strike

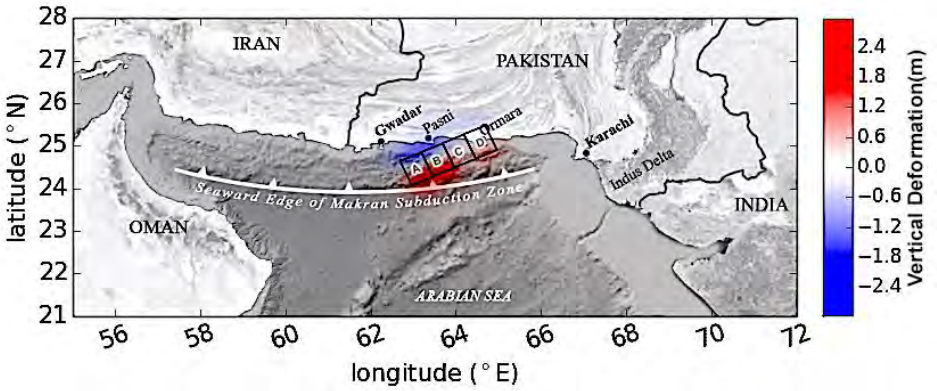

(b) Scenario 2 based on Heidarzadeh and Satake (2014) [5]

Fig. 4 - Sea floor deformation for the two scenarios presented in Table 2. Positive values represent uplift and negative subsidence

3. Results

The grid resolution needed for modelling the tsunami waves within the regional computational domain is both spatially and temporally dependent [21]. Hence for efficient modelling to determine current speeds within Karachi Port, we make use of the adaptive mesh refinement (AMR) in GeoClaw. Following previous studies such as that in [21] the domain was resolved over 5 level grids. An example of the GeoClaw simulation for the 1945 Makran tsunami at a particular time for the first two levels can be seen in Fig. 1. The coarse level-1 grid had a resolution of 154 km, which was used for the full simulation domain. To capture the propagating waves, the level-2 grids were refined by a factor of 16 to give a resolution of about 9.63 km. Like inundation modelling, determining precise current speeds also requires fine resolution. As the wave approached the shores of Karachi, the grids were further refined by additional factors of 4, 15 and 8 within Karachi Port area. This gave corresponding resolutions for level-3, 4 and 5 grids that were approximately 2.4 km, 160m and 20m respectively.

Waves were simulated for 10 hrs for the two DEMs and earthquake sources considered in sections 2.1 and 2.2, and was compared against data that was observed by a float-type tide gauge at Karachi Port. According to Neetu et al. (2011) the tide gauge had malfunctioned due to the tsunami and was repaired, thus kept recording the surface elevation during the event. The observation of the water surface elevation in Fig. 6 clearly shows the time the tide gauge malfunctioned i.e. the period where no data has been recorded just before 5 hours. Results show the initial wave at Karachi having an arrival time and wavelength similar to observations, although later waves do not seem to be well captured by the model. Moreover, amplitudes of the initial waves are almost double those observed. The recent bathymetry and the one closer to the event show almost similar pattern for scenarios 1 and 2. The marigram shows the third wave as the highest as opposed to the fourth according newspaper accounts. Further this is also not the case for the model runs where the first wave is the largest. For the single fault source, the third wave has the same wave height as the observed fourth wave although it arrives later.

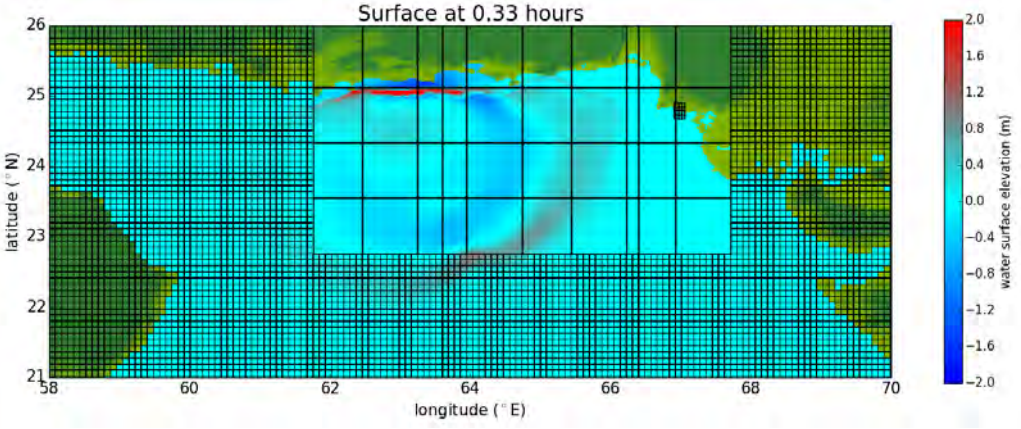

Fig. 5 – A time snapshot of a GeoClaw simulation for the 1945 Makran tsunami showing level-1 grid cells and only grid patches for higher level grids; each patch is up to 60x60 grid cells. Level-2 patches cover part of the Arabian Sea and finer grid patches are also visible only near Karachi.

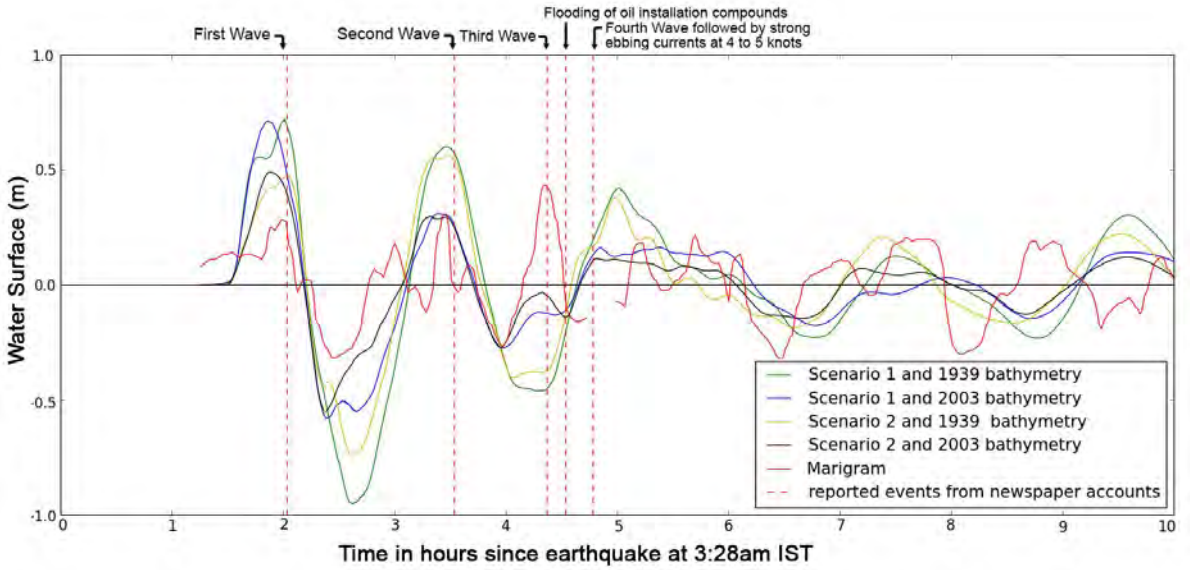

Fig. 6 – Comparison of the observed water surface elevation and the simulated scenarios at Karachi Port for the 1945 Makran tsunami. The dashed red lines give the approximate times of waves and flooding reported in newspaper accounts of the tsunami (details in text).

3.1 Water Surface Elevation, Current Speeds, Velocity Field and Vorticity

Considering the single fault earthquake source, Fig. 7 and Fig. 8 depict four time frames for corresponding water surface elevation, current speeds (overlayed by the velocity field) and the vorticity from 2hrs after the earthquake to 3hrs during which the recession is greatest. The modelling in Fig. 7 uses bathymetry from 1939 charts whereas Fig. 8 uses bathymetric charts from 2012. The figures show that the strongest currents have been calculated when the water is receding and the wave surface elevation is at its lowest. Moreover, it is the 1939 bathymetry over which the strongest currents occur and are between 1.8 to 3 m s^{-1}. This model result corresponds to reports which mention that the strong ebbing currents were between 4-5 knots (2-2.6 ms^{-1}), except the speeds were thought to be a result of the highest wave generated [13]. The receding wave mentioned in Pendse [13,14] was reported to have caused damage within the Karachi harbour. These estimates are important and can then be used to understand the cause of damage in the harbour.

The corresponding velocity field shows huge gyres forming just outside the entrance near the breakwater on the West. The intensity of these circulations can be judged by the vorticity, which is very large over the bathymetry on the 2012 chart. The extension of the breakwater seems to protect the modern day Karachi Port. Moreover, one can observe vortex shedding which can be dangerous. Although the Karachi Port area has been resolved to 20 m this is not enough as seen in the vorticity plots where the boundaries of the patches for vorticity are quite evident. This can be corrected by increasing the resolution to 5m.

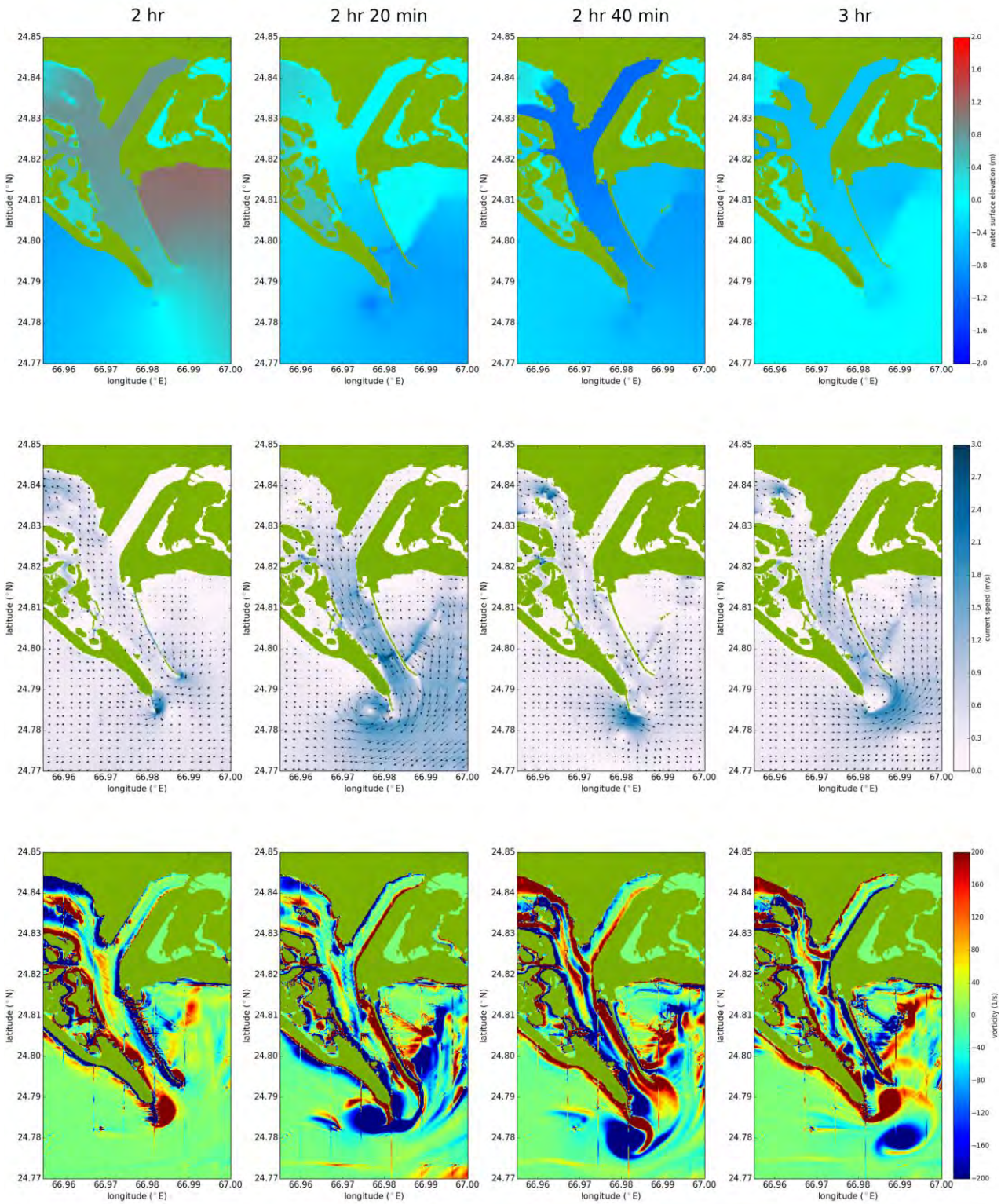

Fig. 7 – Simulated water surface elevation (top row), current speed and velocity field (middle), and vorticity (bottom row) at different times 2 hrs after the earthquake in Karachi Port for bathymetry on a 1939 nautical chart.

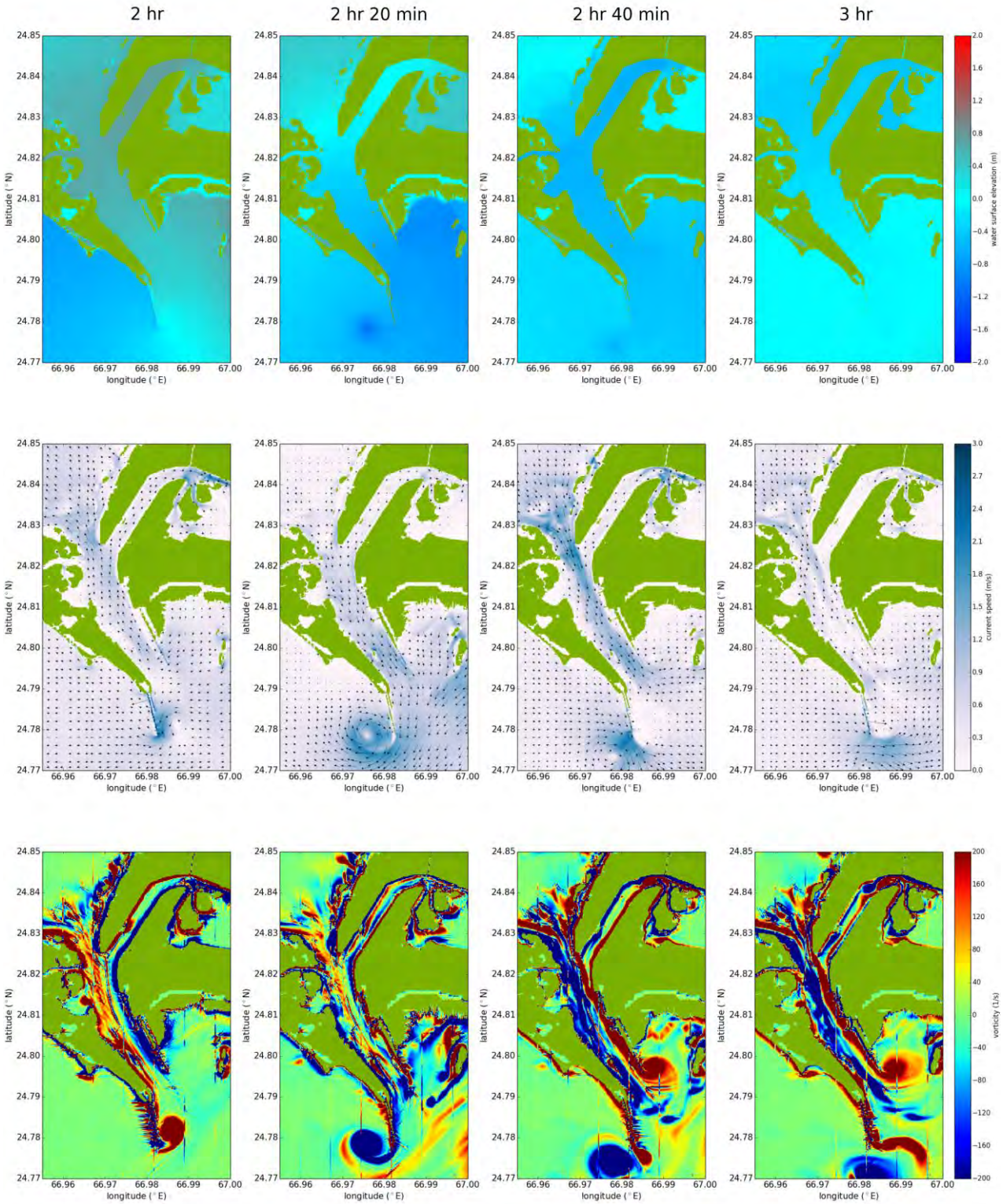

Fig. 8 - Simulated water surface elevation (top row), current speed and velocity field (middle), and vorticity (bottom row) at different times 2 hrs after the earthquake in Karachi Port for bathymetry on a 2012 nautical chart.

3.2 Damage Index

Maximum current speeds in knots and the possibility of damage were derived from GeoClaw output (see Fig. 9 and Fig. 10). The possibility of damage shown in the figures was determined through the application of a damage index developed from tsunami-current measurements in harbours and ports worldwide by Lynett et al. (2012) [15]. What can be assessed from the figures is that the single fault and the 1939 bathymetry in the left panel of Fig. 9 shows quite extensive Minor/Moderate damage possibility around the entrance.

The damage index corresponding to Minor/Moderate damage can result in damage to docks/small boats or large buoys moved. Moreover, it could result in < 25% moderate damage to docks/vessels and/or midsized vessels breaking off their mooring [15]. This result is important as it seems to suggest that the under-repair groyne on the East side of the entrance could have been washed away as reported in newspaper accounts. For the modern bathymetry the damage seems to be contained more around the extended breakwater with the inner harbour being protected. For Fig. 10 where the source consists of four subfaults, the damage seems to be contained.

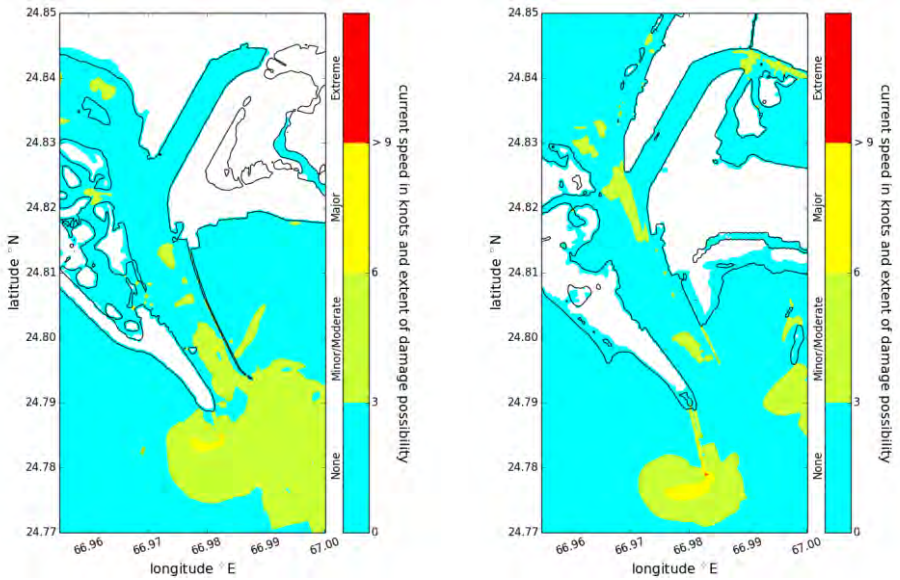

Fig. 9 – Damage index for 1939 (left panel) and 2012 (right panel) charts for a single fault scenario 1.

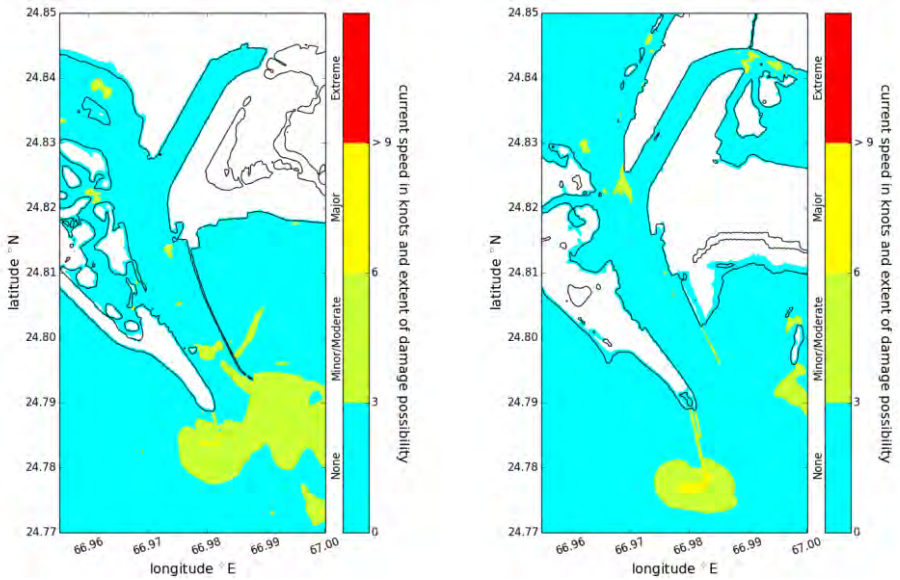

Fig. 10 - Damage index for 1939 (left panel) and 2012 (right panel) charts for a subfault scenario 2.

4. Uncertainties

Section 2.2 simplifies the modeling by excluding submarine landslides as tsunami sources. Submarine mass movements during or soon after the great 1945 Makran earthquake are indicated by reported breaks in a submarine telegraph cable between Karachi and Muscat [8], and the wave train recorded by the Karachi marigram contains short-period waves that are difficult to explain by a simple tectonic source [5–7, 22]. Future research could consider the possible effect of submarine landslides, although there is no indication of exactly where the cable breaks occurred.

Additional uncertainties arise from calibration and bathymetric data. The marigram contains gaps. The tide gauge design did not necessarily ensure full and quick recording of rapid changes in water level. Eyewitness accounts of the tsunami at Karachi [11] contain large discrepancies. Digitizing of nautical charts yielded cells without data, and interpolation into these cells may exaggerate or suppress certain seabed and shoreline features. All these uncertainties may contribute to differences in Fig. 6 between the recorded marigram and the synthetic tide gauge results.

5. Conclusions

The open-source code GeoClaw was used to simulate tsunami arrivals and currents in Karachi Port for comparison with observations of the 1945 Makran tsunami. The comparison incorporated bathymetric data from surveys before 1945. Additional modelling, using newer bathymetry, explored potential effects on today's Karachi Port.

The simulations incorporate simplifying assumptions about sources for the 1945 tsunami. The modelled sources are purely tectonic, and as in other Makran tsunami simulations the fault planes strike obliquely to the likely plane of the Makran subduction thrust. The modelled sources do not include submarine slides or splay faults.

Results show the initial wave at Karachi having an arrival time and wavelength similar to observations. Subsequent waves are not as well captured by the model, but there are also discrepancies between a marigram and newspaper accounts in the time and relative size of the fourth wave. Amplitudes of the initial waves in the simulations are almost double those observed.

Further, results showed the strongest of the currents existed when the water is receding and the wave surface elevation is at its lowest. Moreover, it is the 1939 bathymetry over which the strongest currents occur and are between 1.8 to 3 m s^{-1}. This observation corresponds to reports which mention that the strong ebbing currents were between 4-5 knots (2-2.6 ms^{-1}), except the speeds were thought to be as a result of the highest wave generated [13]. The receding wave is reported to have caused damage within the Karachi harbour.

The simulated velocity field shows huge gyres forming just outside the entrance near the breakwater on the West. The intensity of these circulations can be judged by the vorticity, which is very large over the 2012 bathymetry. The extension of the breakwater seems to protect the modern day Karachi Port. Moreover, one can observe vortex shedding which can be dangerous to structures. Although the Karachi Port area has been resolved to 20 m this is not enough as seen in the vorticity plots, where the boundaries of the patches for vorticity are quite evident. This can be corrected by increasing the resolution to 5 m.

We also examined whether the current speeds were high enough to cause the kind of damage that was done within Karachi port. Application of a damage index previously developed from tsunami-current measurements in harbours and ports worldwide [15] helped establish that for a single fault source and the 1939 bathymetry the Minor/Moderate damage was extensive, suggesting the under repair groyne could have washed away. Further, the extension of the breakwaters limits the damage outside, especially in the vicinity of the breakwater.

6. Acknowledgements

Brian F. Atwater provided historical maps and manuscript reviews. Capt. Syed Mushtaq Ali helped us acquire modern day nautical charts for Karachi Harbour without which simulations for the Port would not have been possible. United Nations Economic and Social Commission for Asia and the Pacific for its support of the UNESCO Makran projects; Oxfam GB; and USAID's Office of Foreign Disaster Assistance. The support has helped build capacity in Pakistan's Preparedness for tsunamis.

7. Copyrights

8. References

[1] Lynett PJ, Borrero JC, Weiss R, Son S, Greer D, Renteria W (2012): Observations and modeling of tsunami-induced currents in ports and harbors, *Earth and Planetary Science Letters*, **327**, 68–74.

[2] Okal EA, Fritz HM, Raad PE, Synolakis C, Al-Shijbi Y, Al-Saifi M (2006): Oman Field Survey after the December 2004 Indian Ocean Tsunami, *Earthquake Spectra*, **22** (S3), 203–218.

[3] Coulter HW, Migliaccio RR (1966): Effects of the earthquake of March 27, 1964, at Valdez, Alaska, *U.S. Geological Survey Professional Paper*.

[4] Byrne DE, Sykes LR, Davis DM (1992): Great thrust earthquakes and aseismic slip along the plate boundary of the Makran subduction zone, *Journal of Geophysical Research*, **97** (B1), 449–478.

[5] Heidarzadeh M, Satake K (2014): New Insights into the Source of the Makran Tsunami of 27 November 1945 from Tsunami Waveforms and Coastal Deformation Data, *Pure and Applied Geophysics*, **172** (3), 621–640.

[6] Rajendran CP, Ramanamurthy MV, Reddy NT, Rajendran K (2008): Hazard implications of the late arrival of the 1945 Makran tsunami., *Current Science (00113891)*, **95** (12).

[7] Neetu S, Suresh I, Shankar R, Nagarajan B, Sharma R, Shenoi S, Unnikrishnan A, Sundar D (2011): Trapped waves of the 27 November 1945 Makran tsunami: observations and numerical modeling, *Natural Hazards*, 1–10.

[8] Ambraseys NN, Melville CP (1982): *A history of Persian earthquakes*, Cambridge University Press, Cambridge, http://www.loc.gov/catdir/enhancements/fy0632/81015540-t.html.

[9] Hoffmann G, Rupprechter M, Balushi NA, Grützner C, Reicherter K (2013): The impact of the 1945 Makran tsunami along the coastlines of the Arabian Sea (Northern Indian Ocean)–a review, *Zeitschrift für Geomorphologie, Supplementary Issues*, **57** (4), 257–277.

[10] Kakar DM, Naeem G, Usman A, Hasan H, Lodhi HA, Srinivasalu S, Andrade V, Rajendran CP, Beni AN, Hamzeh MA (2014): Elders Recall an Earlier Tsunami on Indian Ocean Shores, *Eos, Transactions American Geophysical Union*, **95** (51), 485–486.

[11] Kakar DM, Naeem G, Usman A, Mengal A, Naderi Beni A, Afarin A, Ghaffari H, Fritz HM, Pahlevan F, Okal EA, Hamzeh MA, Ghasemzadeh J, Al-Balushi NS, Hoffmann G, Roepert A, Seshachalam S, Andrade V (2015): *Remembering the 1945 Makran tsunami: interviews with survivors beside the Arabian Sea.*, UNESCO-IOC Brochure, 79 p., http://iotic.ioc-unesco.org/news/detail/17/remembering-the-1945-makran-tsunami-%E2%80%93-interviews-with-survivors-beside-the-arabian-sea.

[12] Bombay (India : State) (1866): *Kurrachee Harbour Works: Correspondence, from November 1856 to June 1866 : Selected from the Records of Government*, Government at the Education Society's Press, https://books.google.com.pk/books?id=amomkgAACAAJ.

[13] Pendse CG (1946): The Mekran Earthquake of 28th November 1945, *India Meteorological Department - Scientific Notes*, **X** (No. 125), 141–147.

[14] Pendse CG (1946): A short note on the Mekran earthquake of 28th November 1945, *Journal of Scientific and Industrial research*, **5**, 106–108.

[15] Lynett PJ, Borrero J, Son S, Wilson R, Miller K (2014): Assessment of the tsunami-induced current hazard, *Geophysical Research Letters*, **41** (6), 2048–2055.

[16] LeVeque RJ, George DL, Berger MJ (2011): Tsunami modelling with adaptively refined finite volume methods, *Acta Numerica*, **20**, 211–289.

[17] Clawpack Development Team (2015): *Clawpack Software*, http://www.clawpack.org.

[18] Field AM (1935): *BA 40 - Karachi Harbour*, Admiralty, London.

[19] Bhatti CD (2012): *PAK 30 - Karachi Harbour*, Pakistan Navy Hydrographic Department, Karachi, Pakistan.

[20] Page WD, Alt JN, Cluff LS, Plafker G (1979): Evidence for the recurrence of large-magnitude earthquakes along the Makran coast of Iran and Pakistan; Recent crustal movements, 1977, *Tectonophysics*, **52** (1–4), 533–547.

[21] George DL (2013): Modeling Hazardous, Free-Surface Geophysical Flows with Depth-Averaged Hyperbolic Systems and Adaptive Numerical Methods, *Computational Challenges in the Geosciences*, C. Dawson, and M. Gerritsen, eds., Springer New York, New York, NY, 25–48.

[22] Rastgoftar E, Soltanpour M (2016): Study and numerical modeling of 1945 Makran tsunami due to a probable submarine landslide, *Natural Hazards*, **83** (2), 929–945.